

## Reply to reviewers: Shallow Cumulus Cloud Feedback in Large Eddy Simulations - Bridging the Gap to Storm Resolving Models

Jule Radtke, Thorsten Mauritsen, Cathy Hohenegger

We thank the referees for their constructive comments, that have helped to improve the manuscript. In the following, referees' comments are in *italics*, authors' responses are in normal font.

### Anonymous Referee 1

*The authors present a nice, clear and well worked out analysis looking to bridge the LES and convection permitting model scales in regards to subtropical cloud feedbacks.*

We thank the referee for the positive assessment.

*I think it is possibly worth adding to the conclusion 'SRMs may exaggerate the tradewind cumulus cloud feedback' that this for a SRM that is configured with a similar all-or nothing cloud scheme. It is true that most SRMs have an all or nothing scheme, but it would be interesting to get some commentary from the authors on this feature as SRMs become more the norm and include more complex cloud schemes.*

We agree this is worth adding. We rewrote line 257 "Provided the identified resolution-dependence of the cloud amount feedback carries over to other model codes, then it implies that storm resolving models configured with a similar all-or-nothing cloud scheme may exaggerate the trade wind cumulus cloud feedback."

*It would also be good to get a discussion from the others as to why their results point towards a zero cloud feedback in the trade cumulus, while previous studies do not.*

Please note our comment to this point below.

*Ln 29: the parenthetical statement ('unlike climate models') needs to be set off from the rest of the sentence.*

We added that.

*Ln 40: Why allegedly?*

True, we deleted that.

*Ln 76: I think maybe 'idealized'- while sort of technically correct this tends to be in relation to a person's beliefs (<https://www.merriam-webster.com/dictionary/idealistic>)*

Thank you for pointing this out, we modified that.

*Ln 96: Does the trade inversion get set by the large scale forcing imposed on the LES? I see this is discussed later.*

Yes, to clarify this we added in line 96: "... the trade wind inversion .... which develops as a result of the prescribed large scale subsidence."

*Ln 155: In the case of uniform warming I guess the inversion strength is held fixed- so we are only really looking at what is commonly characterized as the SST dependence of subtropical cloud (Klein et al., 2017). I see this is discussed on ln 195, but it might be useful to note this here.*

*Klein, S. A., Hall, A., Norris, J. R., and Pincus, R.: Low-Cloud Feedbacks from Cloud-Controlling Factors: A Review, Surv Geophys, 38, 1307-1329, 10.1007/s10712-017-9433-3, 2017.*

Yes, we added noting this here already with "... a uniform temperature shift, which implies a fixed inversion strength and is commonly characterized as the SST dependence (Klein et al. 2017), ...".

*Fig. 9: why aren't the unifw-P and madw simulations joined with a line?*

Too many lines make the plot quite busy. We think not showing the lines eases the understanding of the plot and makes no difference to its message. Therefore, we hesitate to change this.

*Ln: 240: Can you comment on how much inter-LES differences in resolution might affect their inferred cloud feedback strength, or is there only a sizable shift when convection permitting simulations are examined? Also- on line 260 it is noted that other LES studies have inferred a substantial positive feedback. Can you comment on why these studies ended up with this result and the present study does not?*

This is an inherently difficult question to answer. We added the following speculative text that rounds off the paper: "It is perhaps tempting to think that other LES studies were under-resolved, that is, if they had been run with higher resolutions their estimated cloud feedback might have decreased. Although it seems likely that most LES will exhibit a similar resolution dependence of the cloud amount feedback to that found here, it is not clear why they should all converge to a near-zero total feedback given their differences in e.g. microphysics, and so no conclusions in this regard can be drawn here. It is, however, an interesting question for the community to address in the future."

## **Anonymous Referee 2**

*Review of "Shallow Cumulus Cloud Feedback in Large Eddy Simulations — Bridging the Gap to Storm Resolving Models" by Radtke, Mauritsen and Hohenegger, ACP-2020-1160.*

*Summary:*

*An idealized shallow cumulus case based on the RICO field campaign is simulated at a number of horizontal resolutions with and without idealized warming perturbations. These simulations are performed in a single model, the ICON-LEM. The authors find that cloud fraction in the present day climate are proportional to grid spacing. Similarly, the decrease in cloud fraction with idealized warming perturbations is also proportional to grid spacing. The highest resolution simulations suggest (very) small positive cloud feedbacks in response to warming. This result is robust to the inclusion of precipitation and the type of warming perturbation, i.e., uniform in the vertical or moist adiabatic.*

*Assessment:*

*The paper is focused and clearly written and illustrated with figures. I have only minor suggestions, mostly related to additional references and clarifications.*

*Recommendation: Minor revisions.*

We thank the referee for the positive assessment.

*Minor comments/additional references:*

1. *Blossey et al (2009, JAMES, <https://doi.org/10.3894/JAMES.2009.1.8>) also includes a study of the effect of changes in horizontal and vertical grid spacing on shallow cumulus clouds in two dimensional simulation across a similar range of resolutions as in the present paper. See in particular section 4 and figure 8 of that paper. Those simulations were based on composite low cloud regimes from a superparameterized global simulation and sought to understand the robustness of a negative low cloud feedback in that model. While the sign of the cloud response to warming was different in that setting, the same message emerged as in the present paper: higher resolution led to smaller cloud fractions and a weaker cloud response to warming in one of the cases considered in that paper. The setup in those simulations was more complicated than here, including an adaptive large-scale vertical velocity based on the weak temperature gradient approximation.*

Thank you for drawing our attention to that reference, we added in line 259: "Blossey et al. (2009), who also included a study of the effect of grid spacing on shallow cumulus clouds in two dimensional simulations, came to the same conclusion, while the setup was more complicated and the sign of the cloud response to warming was different: at higher resolution cloud fractions are smaller and the cloud response to warming weaker."

2. *I didn't understand from the paper whether the RRTM radiation computation was offline, meaning that the fluxes were computed but the heating rates not applied to the ICON LEM fields, or online, meaning that they were. The description on p3/l68-69 suggests that they were offline, because the Van Zanten et al large-scale forcings (which in part represent radiative heating) are applied in the boundary layer. I would ask the authors to make this distinction clear in the text and also to refer the reader to the appendix for more details. Whether the*

*radiation computation is online or offline, the results of the paper are worth publishing. If longwave radiative heating is not included in the simulations, I would ask the authors to mention Narenpitak and Bretherton (2019, JAMES,<https://doi.org/10.1029/2018MS001572>) who found a negative shallow cumulus feedback that was driven in part by stronger LW cooling of the trade cumulus BL in a warmer climate. See also Wyant et al (2009, JAMES, <https://doi.org/10.3894/JAMES.2009.1.7>) who earlier hypothesized this mechanism. Narenpitak and Bretherton also considered two resolutions, 100m and 4km, in their simulations.*

Thank you for recommending the references. Our RRTM radiation was computed online, we clarify this in line 67-70: "As modification to the case defined by van Zanten et al. (2011), radiation is computed interactively online to be able to calculate cloud radiative effects ... Below 4 km height, initial profiles and large scale forcings as in van Zanten et al. (2011), besides the radiative cooling, are applied, above they are expanded accordingly, mostly with piecewise linear extrapolation, see Appendix A1 for details."

*Specific comments (3/58 means p. 3, line 58):3/58:*

*It would be useful to the reader to know what cloud droplet number and/or aerosol concentration was specified for the precipitating simulations. This could be moved to the appendix if necessary.*

We corrected and clarified in line 58: "In experiments with precipitation processes a one-moment microphysics scheme including cloud water, rain, snow and ice with a constant cloud droplet concentration of  $200 \text{ cm}^{-3}$  (Doms et al., 2011) is applied."

*5/106 Would it be worth citing Cheng et al (2010, JAMES, <https://doi.org/10.3894/JAMES.2010.2.3>) who looked at the effect of differing horizontal resolution in the present day setting? If there are multiple studies along these lines, it could be phrased as "(e.g., Cheng et al, 2010)".*

Thank you for recommending this reference. We rewrote line 106/107: "Most importantly, we note that at coarser resolutions cloud cover is substantially enhanced (Fig. 2). This was similarly found in e.g. Cheng et al (2010)."

*7/123-130: Is there a good reference that talks about the changes in mixing in shallow clouds as resolution decreases?*

We are not aware there is a good reference.

*8/139: It might be worth citing Albrecht (1993, JGR, <https://doi.org/10.1029/93JD00027>) just after "...because it removes moisture available for evaporation near the inversion.*

We added that.

*"10/180-188: I would suggest using the phrases "cloud amount feedback" and "cloud optical depth feedback" here, as is done later in the paper.*

We followed this suggestion and rewrote lines 180-188: "This is due to a compensating cloud optical depth feedback ... In contrast to the cloud amount feedback, though, the cloud optical depth feedback is not strongly resolution dependent."

*11/194: The uniform warming perturbation implies a negative change in EIS from present day to warmed climate. Following the climatological fit of Wood and Bretherton(2006), this would imply a decrease in cloud fraction is expected (if one assumes a similar relationship in a future climate). However, the response of this particular case does not seem to follow that prediction. This is just a comment and doesn't need to be acknowledged in the paper.*

Thank you for this comment.

*14/259-262: Presumably the shallow cumulus feedback will be an aggregate feedback over a number of cloud regimes, weighted by the frequency of occurrence of those cloud regimes (which itself could change with climate). The case presented in this paper predicts the cloud response in one of those cloud regimes. If the high-resolution cloud fraction and/or SWCRE differ from the observed mean in shallow cumulus regions, would the near-zero cloud feedback predicted by the present study be expected to carry over to those other regimes?*

There is ample evidence that stratocumulus and trade wind cumulus clouds behave differently to warming, and so we do not think stratocumulus clouds will exhibit a near-zero cloud feedback given sufficient resolution. Other regimes such as mid- and high latitude shallow cumulus or fair weather cumulus over land may be more similar to the regime studied here, but we prefer to not speculate on this point.

*15/282: It would be good to be explicit that  $\partial_t \Theta$  in the table is equivalent to  $Q_R$  here in the text. The caption to the table also uses a small  $\theta$  in  $\partial_t \theta$ , while the table header uses  $\Theta$ . It would be good to be consistent.*

Thank you for pointing out this inconsistency, we adapted this.

*Typographical suggestions:*

*7/136-137: suggested rephrasing: "... are very similar, the inversion height in the precipitating case with 500m and 5km resolution is around 150m and 350m lower, respectively, than in the non-precipitating case ...". I felt like this wording would be easier for the reader to follow.*

Thank you for this suggestion. We followed the suggested rephrasing.

*12/212: Suggested re-wording: "... responds to warming in both precipitating and non-precipitating simulations." I think that the emphasis on "both" is helpful for the reader.*

Thank you for pointing this out. We followed the suggested re-wording.

*14/253-254: Suggested re-wording: "All in all, the decrease of cloud cover and increase*

*in cloud water with warming compensate and result in convergence to a near-zero trade wind cloud feedback at high resolution in these simulations."*

We followed the suggested re-wording.

# Shallow Cumulus Cloud Feedback in Large Eddy Simulations - Bridging the Gap to Storm Resolving Models

Jule Radtke<sup>1,2</sup>, Thorsten Mauritsen<sup>3</sup>, and Cathy Hohenegger<sup>4</sup>

<sup>1</sup>Meteorological Institute, Center for Earth System Research and Sustainability (CEN), Universität Hamburg, Hamburg, Germany

<sup>2</sup>International Max Planck Research School on Earth System Modelling, Max Planck Institute for Meteorology, Hamburg, Germany

<sup>3</sup>Department of Meteorology, Stockholm University, Stockholm, Sweden

<sup>4</sup>Max Planck Institute for Meteorology, Hamburg, Germany

**Correspondence:** Jule Radtke (jule.radtke@uni-hamburg.de)

**Abstract.** The response of shallow trade cumulus clouds to global warming is a leading source of uncertainty ~~to interpretations and in~~ projections of the Earth's changing climate. A setup based on the Rain In Cumulus over the Ocean field campaign is used to simulate a shallow trade wind cumulus field with the Icosahedral Non-hydrostatic Large Eddy Model in a control and a perturbed ~~4K warmed~~~~4K warmer~~ climate, while degrading horizontal resolution from 100 m to 5 km. As the resolution is

5 coarsened the ~~basic base~~ state cloud fraction increases substantially, especially ~~at near~~ cloud base, lateral mixing is weaker and cloud tops reach higher. Nevertheless, the overall vertical structure of the cloud layer is surprisingly robust across resolutions. In a warmer climate, cloud cover reduces, alone constituting a positive shortwave cloud feedback: the strength correlates with the amount of ~~basic base~~ state cloud fraction, thus is stronger at coarser resolutions. Cloud thickening, resulting from more water vapor availability for condensation in a warmer climate, acts as a compensating feedback, but unlike the cloud cover 10 reduction it is largely resolution independent. Therefore, refining the resolution leads to convergence to a near-zero shallow cumulus feedback. This dependence holds in experiments with enhanced realism including precipitation processes or warming along a moist adiabat instead of uniform warming. Insofar as these findings carry over to other models, they suggest that storm resolving models may exaggerate the trade wind cumulus cloud feedback.

## 1 Introduction

15 How shallow cumulus clouds respond to global warming has been recognized as a critical source of uncertainty to process- or model-based estimates and interpretations of the Earth's changing climate (~~Bony and Dufresne, 2005; Vial et al., 2013; Zelinka et al., 2020~~  
~~Bony and Dufresne, 2005; Vial et al., 2013; Zelinka et al., 2020; Flynn and Mauritsen, 2020; Sherwood et al., 2020~~). Most frequently shallow cumulus clouds are observed in the ~~tropical~~ trade wind region and thus often called trade-wind cumuli, even if they appear in most regions on Earth. Due to their widespread occurrence over the world's oceans, shallow cumuli are, though 20 small in size, crucial to the Earth's radiative balance and act to cool the Earth by reflecting shortwave radiation (Hartmann et al., 1992). Their response to global warming is therefore important for the global-mean cloud feedback. Actually, it is their

25 differing response to warming that explains much of the disagreement in climate sensitivity across climate models (Bony and Dufresne, 2005; Webb et al., 2006; Vial et al., 2013; Boucher et al., 2013; Medeiros et al., 2015; Zelinka et al., 2020; Flynn and Mauritsen, 2020). Most global climate models (GCMs) simulate a positive low cloud feedback primarily due to reduction of cloud cover in response to warming. In models probed in the fifth phase of the Coupled Model Intercomparison Project (CMIP5) the low-level cloud feedback varies between 0.16 to 0.94  $\text{W m}^{-2}$  with most spread coming from the low-cloud amount feedback, the latter with values ranging between -0.09 and 0.63  $\text{W m}^{-2}$  (Boucher et al., 2013; Zelinka et al., 2016).

30 Emerging tools to advance understanding are global high resolution models that ~~–~~ unlike climate models ~~–~~ explicitly simulate convective motions instead of parameterizing them (Stevens et al., 2020). In past studies of shallow cumulus clouds and their response to a warmer climate mostly large eddy (~~hectometer-resolving~~) simulations (LES) ~~have been used~~ ~~resolving hectometer scale motions have been applied~~ (Rieck et al., 2012; Blossey et al., 2013; Bretherton et al., 2013; Vogel et al., 2016; Stevens et al., 2001; Siebesma et al., 2003; van Zanten et al., 2011). LES is a turbulence modeling technique in which most 35 of the energy containing motions are explicitly resolved, but because of their computational expense LES studies have been limited in their domain size and timescales. Due to increasing computational power, it has become possible to run simulations on global domains, albeit ~~not at hectometer but at~~ kilometer scales (e.g. Tomita, 2005; Stevens et al., 2019). These models are often called cloud resolving or convection permitting models (Prein et al., 2015) but here referred to as storm resolving models (SRMs) following Klocke et al. (2017) and Stevens et al. (2019); see also Satoh et al. (2019) for a discussion of naming. Global SRMs provide the opportunity to study cloud feedbacks without having to rely on an uncertain convective parameterization 40 and while interacting with the large scale environment, but at a typical grid spacing of a few kilometers shallow convection ~~is allegedly remains~~ poorly resolved.

45 This study aims to bridge the gap between findings based on limited-area large eddy simulations that typically use hectometer or finer grid spacings and emerging global storm resolving models that apply kilometer grid spacings. It investigates how the representation of shallow cumuli and their climate feedback is affected by the choice of horizontal resolution. To do so a setup based on the Rain In Cumulus over the Ocean field campaign is used (Rauber et al., 2007). A shallow trade cumulus field is simulated with the Icosahedral Non-hydrostatic Large Eddy Model (Dipankar et al., 2015; Heinze et al., 2017) in a control and a perturbed ~~4K-4K~~ warmed climate while degrading horizontal resolution from 100 m to 5 km. The results are discussed by initially looking at the effect of resolution on the representation of shallow cumulus clouds in a control climate in Sect. 3, 50 subsequently on the response of shallow cumulus clouds to a warming climate in Sect. 4.

## 2 Model and Setup

Experiments are conducted with the ICOsahedral Non-hydrostatic Large Eddy Model (ICON-LEM). ICON was developed in collaboration between the Max Planck Institute for Meteorology and the German Weather Service and solves the equations of motions on an unstructured triangular Arakawa C grid. For global applications, it is based on successive ~~refinement~~

55 refinements of a spherical icosahedron (Zängl et al. 2015), but here instead a two-way cyclic torus domain is used. A detailed description of the LES version ICON-LEM can be found in Dipankar et al. (2015). In the specific ICON-LEM setup for this study subgrid scale turbulence is modeled based on the classical Smagorinsky scheme with modifications by Lilly (1962). For microphysical properties, the simple saturation adjustment scheme is used in experiments where precipitation is prohibited. In experiments with precipitation processes ~~the two-moment mixed-phase microphysics scheme of Seifert & Beheng (2006)~~ 60 a one-moment microphysics scheme including cloud water, rain, snow and ice with a constant cloud droplet concentration of 200 cm<sup>-3</sup> (Doms et al., 2011) is applied. Radiation is computed with the Rapid Radiation Transfer Model scheme (RRTM, Mlawer et al. 1997). A simple all-or-nothing scheme is applied for cloud fraction (Sommeria & Deardorff 1977).

65 The setup is based on the Rain In Cumulus over the Ocean (RICO) measurement campaign (Rauber et al., 2007). The RICO case developed by van Zanten et al. (2011) prescribes large scale forcings and initial profiles characteristic of the broader trades and serves as a control experiment representative of present climate conditions. Figure 1 shows the profiles used for initialization of potential temperature  $\theta$ , specific humidity  $q_v$  and the horizontal winds  $u$  and  $v$ . The large scale forcing is prescribed with time-invariant profiles of the subsidence rate and temperature and moisture tendencies due to radiative cooling and horizontal advection. As modification to the case defined by van Zanten et al. (2011), radiation is computed interactively online to be able 70 to calculate cloud radiative effects, which requires a model top of about 20 km in ICON-LEM. Below 4 km height, initial profiles and large scale forcings as in van Zanten et al. (2011), besides the radiative cooling, are applied, above they are expanded accordingly, mostly with piecewise linear extrapolation, see Appendix A1 for details. Sea surface temperature is fixed at 299.8 K as in the RICO set-up, and bulk aerodynamics formulas parameterize the surface momentum and thermodynamic fluxes. Simulations are performed on a pseudo-Torus grid with doubly periodic boundary conditions and flat geometry. The domain is 75 fixed over a central latitude of 18°N. In the vertical 175 levels are used with grid spacings of 40 to 60 m beneath 5 km height stretching to approximately 300 m at the model top of 22 km. Duration of the simulations is 48 hours and statistics shown are the second day mean.

80 The warming experiment design follows a simple idealistic idealized climate change as used in e.g. Rieck et al. (2012). It increases the temperature profile compared to the control run while keeping relative humidity constant. Simulations are run with five different horizontal resolutions, 100 m, 500 m, 1 km, 2.5 km and 5 km, employed on three different domain sizes. The domain sizes are chosen to be ideally suitable to run with two different horizontal resolutions. They span 50 to 200 points resulting in domain sizes between 12 x 12 km and 500 x 500 km. The basic experiment inhibits precipitation and warms surface and atmosphere uniformly by 4 K as in Rieck et al. (2012). Furthermore two refined experiments are conducted, one allowing 85 precipitation to develop ~~(e.g. as in Vogel et al., 2016)~~as in Vogel et al. (2016), and another one altering the vertical warming to follow a moist adiabat ~~(e.g. as in Blossey et al., 2013)~~as in Blossey et al. (2013). These tests show how robust the findings are against simplifications made in the original experimental setup. See Table 1 for an overview of the different experiments.

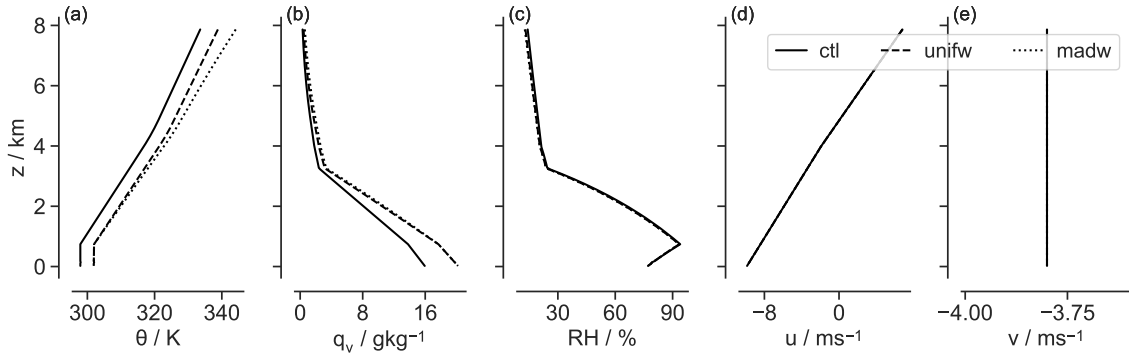


**Figure 1.** Initial profiles of (a) potential temperature  $\theta$ , (b) specific humidity  $q_v$ , (c) relative humidity  $RH$ , (d-e) horizontal winds  $u$  and  $v$  for the control (solid line) and the perturbed (vertically uniform warming, dashed line and warming following a moist adiabat, dotted line) climate states.

**Table 1.** Specifications used for the different perturbation experiments. Specific humidity in the perturbed runs (unifw and madw) is adjusted to keep the relative humidity constant compared to the control simulation.

Hor. Resolution	Hor. Domain	Gridpoints	Temp profile	Prec	Casename
100m	12.6 x 12.6 km <sup>2</sup>	126 <sup>2</sup>	control	no, yes	100m.ctl, -P
			+ 4 K	no, yes	100m.unifw, -P
			+ 4 K moist adiabatic	no	100m.madw
500m	50 x 50 km <sup>2</sup>	100 <sup>2</sup>	control	no, yes	500m.ctl, -P
			+ 4 K	no, yes	500m.unifw, -P
			+ 4 K moist adiabatic	no	500m.madw
1km	50 x 50 km <sup>2</sup>	50 <sup>2</sup>	control	no	1km.ctl
			+ 4 K	no	1km.unifw
2.5km	500 x 500 km <sup>2</sup>	200 <sup>2</sup>	control	no	2.5km.ctl
			+ 4 K	no	2.5km.unifw
			control	no, yes	5km.ctl, -P
5km	500 x 500 km <sup>2</sup>	100 <sup>2</sup>	+ 4 K	no, yes	5km.unifw, -P
			+ 4 K moist adiabatic	no	5km.madw
<i>Additional sensitivity experiment:</i>					
1km	500 x 500 km <sup>2</sup>	500 <sup>2</sup>	+ 4 K	no	large

### 3 Basic state dependency on resolution

In this Section we present characteristics of the simulated shallow cumulus regime in the control case and highlight similarities 90 and differences as the resolution is coarsened. This lays out the ground to study in the following how shallow cumulus clouds respond to a perturbed warmer climate and how this depends on horizontal resolution in Sect. 4.

#### 3.1 Standard Case

At 100 m resolution a typical trade wind cumuli field is simulated that is in line with the range of LES analyzed in the RICO LES intercomparison case (van Zanten et al., 2011). Total cloud cover is 15 % (Fig. 2) which is slightly lower than the cloud 95 cover of 17 % observed during the RICO field study (Nuijens et al., 2009) and the ensemble mean cloud cover of 19 % in the RICO intercomparison case (range 9 - 38 %). The vertical structure is consistent with the general picture of trade wind cumuli cloud layers (Fig. 3). Cloud fraction peaks at cloud base (6 %) near 700 m, then decreases sharply with height, thereafter keeping a value of about 2% through the cumulus layer until 2 km (Fig. 3). Above this height, cloud fraction increases again due to detrainment at cloud top before declining sharply under the trade inversion at around 2.5 km height, [which develops as](#) 100 [a result of the prescribed large scale subsidence](#). Temperature increase and sharp humidity decrease mark the inversion and top of the cloud layer.

At coarser resolutions the overall structure of the boundary [layer](#) and cloud layer is surprisingly similar to the 100 m resolution simulation. The vertical structure of cloud fraction is in all experiments characterized by a dominant peak at cloud base 105 and a second smaller peak near the inversion (Fig. 3). Therefore, at all resolutions cloudiness at cloud base contributes most to total cloud cover. All experiments simulate a well-mixed subcloud layer, a transition layer which is most evident in the moisture gradients, a cloud layer, and an inversion layer into which the clouds penetrate and detrain (Fig. 4). However, at coarser resolutions the transition layer is more pronounced exhibiting a stronger moisture gradient and the inversion height is more distributed in the vertical. These variations translate into the most notable differences between the resolutions.

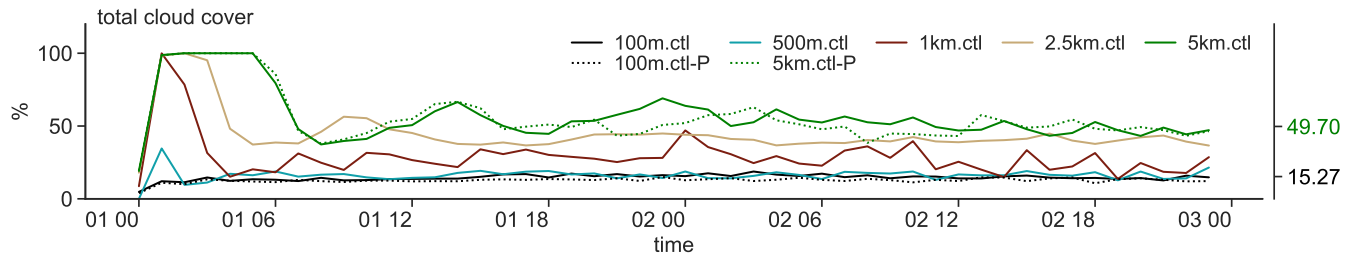


**Figure 2.** Temporal evolution of total cloud cover in ctl at 100 m, 500 m, 1 km, 2.5 km and 5 km resolution (solid lines) and ctl-P at 100 m and 5 km resolution (dotted lines). Ordinates on the right axis display the second day domain averaged total cloud cover for 100m.ctl and 5km.ctl (see Table 2 and 3 for more statistics).

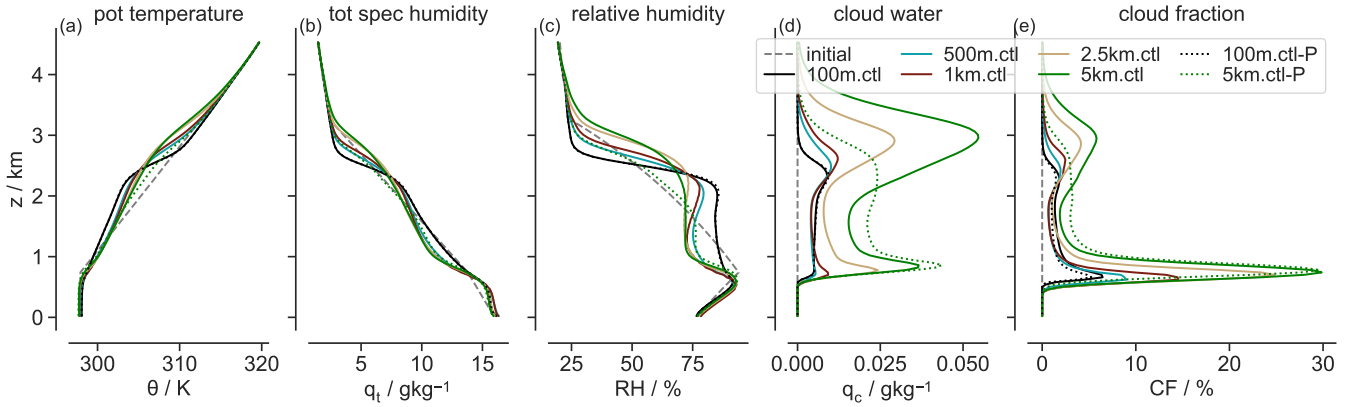


**Figure 3.** Profiles of second day domain averaged (a) potential temperature  $\theta$ , (b) total water specific humidity  $q_t$ , (c) relative humidity  $RH$ , (d) cloud water  $q_c$  and (e) cloud fraction  $CF$  for different horizontal resolutions of the ctl (solid lines) and ctl-P simulations (dotted lines).

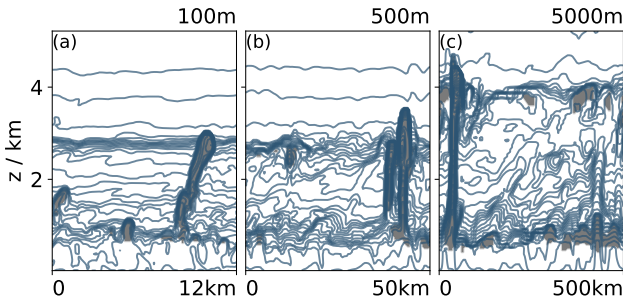


**Figure 4.** Cross section (note the different horizontal extent) of total water specific humidity field and cloud cover at 42 hours simulation time in the ctl simulations for three different horizontal resolutions: (a) 100 m, (b) 500 m, (c) 5 km. The total water specific humidity field is shown as contours evenly spaced every  $0.5 \text{ g kg}^{-1}$  and cloud fraction is grey shaded.

110 Most importantly, we note that at coarser resolutions cloud cover is substantially enhanced (Fig. 2). [This was similarly found in e.g. Cheng et al. \(2010\)](#). At 5 km resolution total cloud cover is more than three times higher than at 100 m (50 vs 15 %). This increase in cloud cover is mostly due to enhanced cloudiness at cloud base and to a smaller extent [from to](#) an increase in cloud fraction near the inversion (Fig. 3). The ratio between cloudiness at cloud base and total cloud cover rises from 0.4 with the 100 m to 0.6 with the 5 km resolution, that is, cloud base cloud fraction contributes more to total cloud cover in the 115 coarser resolution simulations. Further, at coarser resolutions clouds reach higher (Fig. 3). At 5 km resolution clouds deepen up to an inversion height of about 3.2 km, [which is](#) around 700 m higher than at the finest resolution. Both characteristics can be confidently linked to resolution and not domain size as a sensitivity experiment shows (see Appendix B1).

120 Larger cloud cover and higher cloud tops at coarser resolutions can be attributed to weaker small-scale mixing. At coarse resolutions the subcloud layer ventilates less efficiently and the subcloud and cloud base [layer layers](#) are therefore moister

**Table 2.** Averages of total cloud cover ( $CC$ ), maximum vertical cloud fraction ( $CF_{\max}$ ), liquid water path ( $LWP$ ), surface sensible heat flux ( $SH$ ), surface latent heat flux ( $LH$ ), inversion height ( $z_i$ , representing the location of maximum  $\theta$ -gradients), cloud base height ( $z_b$ , representing the minimum height where 50 % of  $CF_{\max}$  is reached) and change in the shortwave cloud radiative effect  $\Delta SWCRE$  at 100 m, 500 m and 5 km resolutions in the non-precipitating simulations of the *ctl*, *unifw* and *madw* climate states.

Case	$CC$	$CF_{\max}$	$LWP$	$SH$	$LH$	$z_i$	$z_b$	$\Delta SWCRE$
	%	%	$gm^{-2}$	$Wm^{-2}$	$Wm^{-2}$	m	m	$Wm^{-2}$
100m	<i>ctl</i>	15.27	6.46	12.06	4.49	153.57	2560	610
	<i>unifw</i>	14.28	6.11	13.65	3.40	199.86	2810	670
	<i>madw</i>	14.24	6.21	13.42	3.31	190.61	2660	640
500m	<i>ctl</i>	16.60	8.94	13.70	5.79	140.81	2760	570
	<i>unifw</i>	13.22	6.90	15.77	4.85	182.75	3090	600
	<i>madw</i>	13.56	7.08	16.02	4.58	174.74	2810	580
5km	<i>ctl</i>	51.21	29.85	86.54	7.26	149.09	3240	610
	<i>unifw</i>	42.36	23.69	90.52	6.33	180.51	3570	640
	<i>madw</i>	43.30	24.38	84.62	5.70	177.61	3180	620

and cooler and as a result associated with stronger surface sensible but weaker latent heat fluxes (Table 2). Moister and colder conditions are consistent with weaker cumulus massfluxes and weaker entrainment of warm dry air from aloft. Because conditions are moister and colder in the boundary layer, relative humidity is enhanced and saturation is more likely [to occur](#), leading to more widespread cloud formation at coarser resolutions. Hohenegger et al. (2020) found similar characteristics in global simulations with explicit convection and grid spacings ranging between 2.5 and 80 km.

125

Additionally, at coarser resolutions small-scale lateral mixing between cumulus clouds and their environment is markedly weaker which explains the higher cloud tops. Figure 5 displays the fractional entrainment and detrainment rates as a measure for lateral mixing intensity diagnosed after Stevens et al. (2001). The entrainment rate at 100 m resolution decreases from 130 2  $km^{-1}$  near cloud base to 1.2  $km^{-1}$  in the cloud layer, which is similar to the rates found in the RICO LES intercomparison case (van Zanten et al., 2011). At 500 m resolution the mean entrainment rate in the cloud layer is around 0.8  $km^{-1}$ , in 5 km around 0.4  $km^{-1}$ , thus notably weaker [than at the finest resolution](#). This might be attributed to larger cloud structures that offer less surface area for dilution compared to smaller cloud structures that are resolved at finer resolutions. Because they dilute less, clouds retain more buoyancy and reach higher at coarser resolutions.

135 **3.2 Precipitating Case**

Trade wind cumulus clouds rain frequently as observations show (Nuijens et al., 2009). We activate precipitation processes to test if the identified resolution dependence is robust in simulations with 100 m, 500 m and 1 km horizontal resolution.

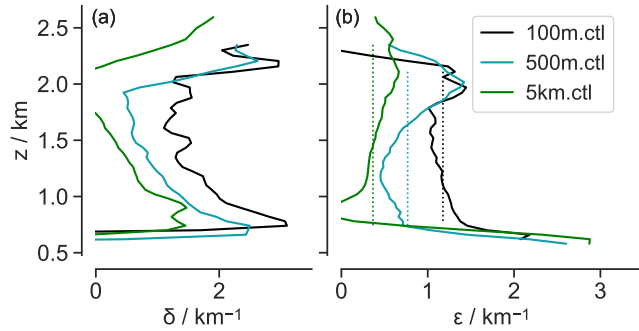


**Figure 5.** (a) Fractional entrainment ( $\varepsilon$ ) and (b) detrainment rate ( $\delta$ ) at 100 m, 500 m and 5 km resolution in CTL. The mean entrainment rate in the cloud layer is shown as dotted lines.

We find that including precipitation processes mainly acts to limit cloud layer deepening. Whereas the 100 m resolution simulations are very similar, with 500 m resolution the inversion height in the precipitating case is around 150 with 500 m and with 5 km around resolution is around 150 m and 350 m lower, respectively, than in the non-precipitating case (Table 3). In the RICO LES intercomparison case van Zanten et al. (2011) also found that precipitating simulations with 100 m resolution cause an approximate 100 m reduction in the depth of the cloud layer. Precipitation acts to limit cloud layer deepening because it removes moisture available for evaporation near the inversion (Albrecht, 1993). The precipitating cloud field is therefore also characterized by less cloud fraction near the inversion (Fig. 3).

**Table 3.** As in Tab. 2 but for the precipitating simulations (P) of the CTL and +4K climate states.

Case	$CC$ %	$CF_{\max}$ %	$LWP$ gm <sup>-2</sup>	$SH$ Wm <sup>-2</sup>	$LH$ Wm <sup>-2</sup>	$z_i$ m	$z_b$ m	$\Delta SWCRE$ Wm <sup>-2</sup>
100m	ctl-P	13.09	5.26	12.88	4.54	154.02	2580	610
	unifw-P	12.38	4.72	13.62	3.42	200.05	2810	670
500m	ctl-P	13.58	6.64	11.93	6.70	139.90	2630	580
	madw-P	10.95	5.37	12.98	6.57	182.14	2780	610
5km	ctl-P	49.63	29.59	55.73	7.95	147.10	2860	660
	madw-P	44.91	25.61	51.57	7.69	180.05	2980	690
								5.2

145

Furthermore, we find that the precipitating cloud fields exhibit more cloud fraction in the lower parts-part of the cloud layer as compared to the non-precipitating cloud field (Fig. 3). Vogel et al. (2016) and van Zanten et al. (2011) both found a similar increase in cloud fraction and explained it by increased evaporation from precipitation concentrated in the cloud layer, noting 150 that the evaporation of precipitation must not be confined to the subcloud layer. Due to this moistening, latent heat fluxes are moderately weaker, e.g. at 5 km around 2 Wm<sup>-2</sup> (compare Tab. 2 and Tab. 3). Additionally, evaporation of falling raindrops

induces a cooling in the subcloud layer, which results in stronger surface sensible heat fluxes.

Because liquid is removed through precipitation, and clouds are shallower, the precipitating simulations have a lower total  
155 cloud cover than the non-precipitating simulations at all resolutions (15 vs 13% at 100 m, 16.6 vs 13.6% at 500 m, 51.2 vs 49.7% at 5 km; Tables 2 and 3). However, changes between the non-precipitating to precipitating cloud ~~field-fields~~ are small and additionally similar across resolution. Therefore, the resolution ~~dependencies remain dependency remains~~ dominant in the precipitating case~~as in the non-precipitating case~~: cloud cover is substantially enhanced and clouds are deeper at coarser resolutions.

## 160 4 Cloud response to warming across resolutions

Here, we investigate how the cloud field responds to warming in dependence of resolution. First, the response to a uniform temperature shift, which implies a fixed inversion strength and is commonly characterized as the SST dependence  
165 (Klein et al., 2017), in the standard non-precipitating case is discussed and how the resolution dependence of the basic state cloud field affects the cloud field's response to warming. Second, the robustness of our results are investigated by testing whether warming along a moist adiabat or in the precipitating case alters the response across resolution.

### 4.1 Response to uniform warming

At 100 m resolution we find a slight cloud cover reduction as response to uniform warming in line with earlier LES-based studies (Rieck et al., 2012; Blossey et al., 2013; Vogel et al., 2016). Total cloud cover decreases from 15.3% to 14.3% (Table 2). It seems plausible that drying (Fig. 6), ~~that results resulting~~ from mixing due to the stronger vertical gradient in specific  
170 humidity within the warmer case, could explain much of this reduction in cloud cover (Bretherton, 2015; Brient and Bony, 2013). It has further been suggested that enhanced surface latent heat fluxes enervate convection, deepening the cloud layer and leading to further drying by mixing (Stevens, 2007; Rieck et al., 2012). However, as more refined experiments (Sect. 4.2) do not result in substantial deepening, this process appears to be of secondary importance. The cloud cover reduction on its own constitutes a positive shortwave cloud feedback.

175

Also at coarser resolutions, we find cloud cover reductions as response to uniform warming (Table 2). Across resolutions the cloud layer is drier, cloud cover reduced and cloud tops reach higher (Fig. 7). The magnitude of cloud cover reduction, however, differs: at 100 m resolution total cloud cover reduces by 1% point, whereas at 5 km resolution total cloud cover reduces by roughly 9% points. At coarse resolutions it is distinctly cloud base cloudiness that reduces with warming. This low resolution  
180 behavior is in contrast to the results of previous high resolution LES studies and observations which suggest a relatively invariant cloud base fraction (Nuijens et al., 2014; Siebesma et al., 2003), but is a common feature in global climate model simulations (Brient and Bony, 2013; Brient et al., 2015; Vial et al., 2016)(Brient and Bony, 2013; Brient et al., 2015; Vial et al., 2016; Mauritsen and  
. We find that the strength of cloud reduction correlates well with the amount of cloud cover in the basic state (Fig. 8): The

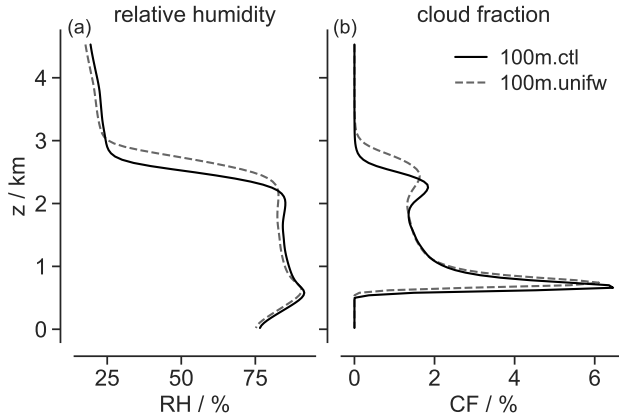


**Figure 6.** Profiles of second day domain averaged (a) relative humidity  $RH$  and (b) cloud fraction  $CF$  for the control (solid line) and vertically uniform warmed (dashed line) simulation at 100 m resolution.

more clouds are present in the basic state, the more cloudiness reduces in the warmer climate. Hence, because cloud cover increases at coarser resolutions, in particular near cloud base, they show a stronger cloud cover reduction than at high resolutions.

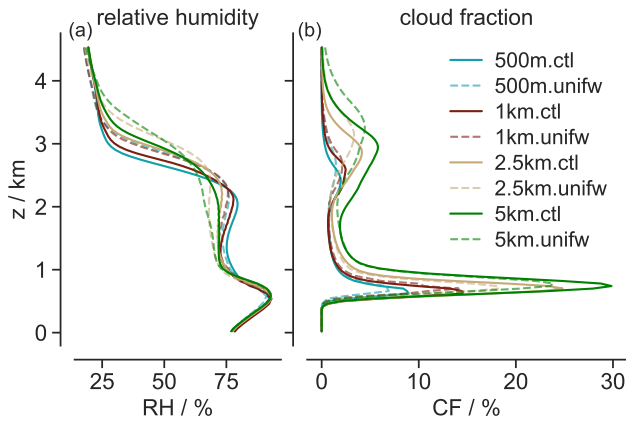


**Figure 7.** As in Fig. 6 but for 500 m, 1 km, 2.5 km and 5 km resolution.

From the reduction in cloud amount, a positive shortwave feedback would be expected, however, the total shortwave feedback at high resolutions is close to zero, e.g. at 100 m with a value of  $0.05 \text{ Wm}^{-2}\text{K}^{-1}$  (Fig. 9). This is due to a compensating   
190 feedback from cloud thickeningcloud optical depth feedback. The cloud liquid water path increases at all resolutions with warming (Fig. 9). Clouds and therefore clouds become more reflective contributing a negative shortwave feedback. In contrast to the cloud amount reduction though, cloud thickening feedback, though, the cloud optical depth feedback is not strongly

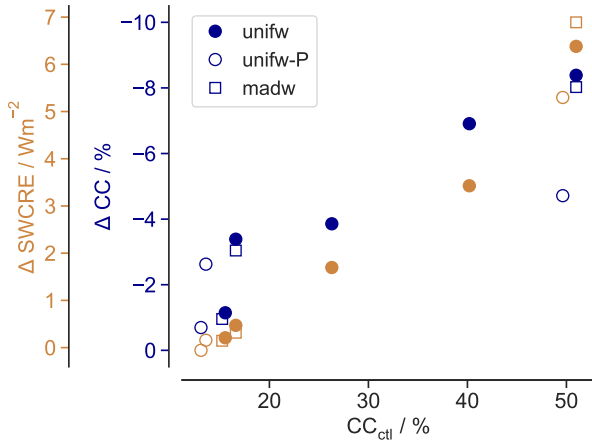


**Figure 8.** Relationship between cloud cover amount in the control simulation ( $CC_{ctl}$ ) and cloud cover reduction with warming ( $\Delta CC$ ) as well as the shortwave cloud radiative feedback ( $\Delta SWCRE$ ) across all simulations.

resolution dependent. An increasing cloud water content with warming is to be expected as more water vapor is available for condensation (Paltridge, 1980); an argument that is not reliant in any meaningful way on resolution. Consequently, the total shortwave feedback shows the same dependence on resolution as the cloud reduction and correlates well with the basic cloud 195 cover, too (Fig. 8). Hence the shortwave cloud feedback is weak or close to zero for high resolution and positive for coarse resolutions.

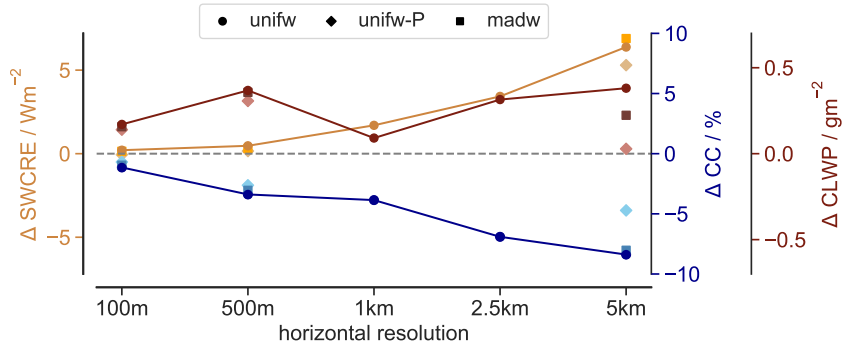


**Figure 9.** Shallow cumulus cloud feedback across resolution: Shortwave cloud radiative feedback  $\Delta SWCRE$ , change in cloud cover amount  $\Delta CC$  and cloud liquid water path  $\Delta CLWP$  between the perturbed warmer and control simulations for all experiments.

## 4.2 Sensitivity of response to refined experimental setups

The base case studied above was admittedly simplistic in that there is no precipitation and a vertically uniform warming was applied. Here we explore the effects of these [simplifying](#) assumptions. The free tropospheric temperature profile in the Tropics is set by the regions of deep convection that are close to a moist adiabat. Therefore, the tropical temperature is expected to warm close to a moist adiabat, leading to more warming aloft than at the surface and has been used in other modelling studies (e.g Blossey et al., 2013; Bretherton et al., 2013). With moist adiabatic warming an increase in dry static stability is introduced: the initial lower tropospheric stability ( $LTS = \theta_{700} - \theta_0$ ) increases from 13.1 K to 14.4 K, and as a result, with moist adiabatic warming the cloud response near the trade inversion is muted (Fig. 10). Both the cloud top height and cloud fraction in the upper regions change only little. The inversion height in the moist adiabatic warming case varies compared to the control case by only around 50 to 100 m, whereas in the uniform warming case the inversion height increased markedly by around 300 m (Table 2). Therefore, cloud deepening is at all resolutions slightly weaker. Nevertheless, total cloud cover reduction is only slightly dampened. (Fig. 9). Overall the changes are small, though, and therefore, the total shortwave cloud radiative feedbacks is only slightly reduced when applying the more realistic warming profile.

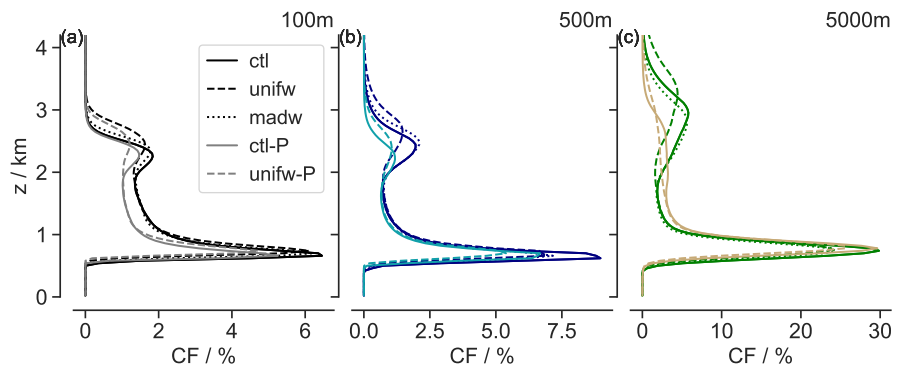


**Figure 10.** Profiles of second day domain averaged cloud fraction at three different horizontal resolutions (a-c) for all experiments.

With precipitation processes activated, the cloud field in a warmer climate responds with a cloud amount reduction across all resolutions, similar to that of the non-precipitating case, though the reductions in total cloud cover are slightly smaller (Tab. 3 vs. Tab. 2). We are aware of two [main mechanism](#) [proposed mechanisms](#) that could be contributing to the dampening. First, precipitation has a constraining effect on cloud deepening, noted by Blossey et al. (2013) and Bretherton et al. (2013). At 500 m resolution the boundary layer deepening with warming is half and at 5 km only a third as much as in the non-precipitating simulations. Therefore, especially near the inversion changes in cloud fraction are reduced (Fig. 10). Second, evaporation of precipitation in the lower cloud layer counteracts drying. Vogel et al. (2016) [who integrated for a longer time period](#) reported likewise that precipitation reduces deepening and drying with warming. In this way, precipitation is thought to promote the robustness of shallow cumulus clouds to warming. Regardless, though, we find the same dependency on resolution of how

shallow cumulus cloud coverage responds to warming ~~as in the~~ ~~in both precipitating and~~ non-precipitating simulations.

To summarize, the different experiments all exhibit the same horizontal resolution dependency on the representation and response of shallow cumulus clouds to warming (Fig. 9). The resolution induced differences are larger than those between 225 the different experimental setups. This confirms that horizontal resolution affects the representation and therewith response of shallow cumulus clouds to warming to first order: the simulated shortwave cloud radiative feedback differs between the resolutions mainly in proportion to the basic state cloud fraction (Fig. 8) and therefore the cloud feedback strength increases at coarse resolutions. Hohenegger et al. (2020) who investigated grid spacings ranging from 2.5 km to 80 km found that cloud 230 cover increases up to 80 km horizontal resolution, which would, provided the results found here carry over also to even coarser resolutions, translate into further increased cloud feedback. At high resolutions, on the contrary, the trade wind cumulus cloud feedback converges to near-zero values in our simulations.

## 5 Conclusions

This study explores the representation and response of shallow trade wind convection to warming and how that depends on horizontal resolution by varying between 100 m and 5 km. Therewith we aim to bridge the gap between findings based on existing 235 large eddy resolving simulations and emerging global storm resolving simulations. Based on the RICO case, simulations representative of trade wind conditions are compared to simulations with a 4 K warmed surface and atmosphere at constant relative humidity, representative of a simple idealized climate change. First, in a basic experiment the representation of shallow trade wind cumuli and their response to a uniformly warmed state is explored. Second, the sensitivity to resolution is probed in refined experimental setups by including precipitation processes and or warming along a moist adiabat in place of uniform 240 warming.

At 100 m resolution a typical trade wind cumuli field is simulated that is in line with observations (Nuijens et al., 2009), and the range of LES analyzed in the RICO intercomparison case (van Zanten et al., 2011). Total cloud cover accounts to 15% in the non-precipitating and 13% in the precipitating case with a prominent peak in all cases near cloud base. At coarser 245 resolutions, cloud cover is substantially enhanced and clouds are deeper; in the most extreme case at 5 km resolution total cloud cover is around ~~3.5~~ three times more extensive. Cloud cover increases mostly due to enhanced cloudiness at cloud base. Weaker subcloud layer ventilation could explain the enhanced cloudiness and a weaker lateral entrainment rate allows the clouds to reach higher. Nevertheless, the overall structure of the boundary and cloud layer ~~bear~~ bears surprising similarity across resolutions explored here, suggesting that, although distorted, the same set of processes act in all cases.

250

In response to warming a cloud reduction can be observed consistently across resolutions. However, whereas at 100 m grid spacing the cloud reduction is rather small, at coarse resolutions the reductions are substantially enhanced. A robust dependency between cloud cover amount and its change with warming emerges: the more clouds are present in the control climate,

the more cloud cover reduces in a warmer climate. Including precipitation processes mainly acts to limit the cloud layer deepening by causing a net warming of the upper cloud layer and thereby stabilising the lower troposphere. A similar effect is found when the warming is done along a moist adiabat. These more refined setups result in nearly constant cloud top height with warming, questioning the idea that a cloud deepening is critical to a positive cloud cover feedback (Rieck et al., 2012). Regardless, the resolution dependence pertaining to ~~cloud cover change~~ the cloud amount feedback is practically the same, also in these less idealized cases. On the contrary, a negative cloud optical depth feedback arises in all simulations due to an increasing cloud liquid water path. Although the magnitude of this feedback varies, there is no obvious dependence on resolution. This is to be expected since increasing amounts of water vapor available for condensation with warming at constant relative humidity is a fundamental physical fact.

All in all, the ~~compensation between the decreasing cloud cover and increasing cloud water with warming results in our ease with convergence towards~~ decrease of cloud cover (positive cloud amount feedback) and increase in cloud water (negative cloud optical depth feedback) with warming compensate and result in convergence to a near-zero trade wind ~~cumulus~~ cloud feedback ~~cloud feedback at high resolution in these simulations~~. Both of these ~~effects~~ feedbacks appear physically appealing: a stronger vertical gradient in specific humidity results in a lowered relative humidity when mixing is activated, and all other things being equal in a slight reduction of the areal fraction where condensation can occur, whereas more availability of water vapor in the boundary layer results in thicker clouds. Provided the identified resolution-dependence of the cloud ~~ever~~ amount feedback carries over to other model codes, then it implies that storm resolving models ~~may exaggerate~~ configured with a similar all-or-nothing cloud scheme ~~may exaggerate the~~ trade wind cumulus cloud feedback. Blossey et al. (2009), who also included a study of the effect of grid spacing on shallow cumulus clouds in two dimensional simulations, came to the same conclusion, while the setup was more complicated and the sign of the cloud response to warming was different: at higher resolution cloud fractions are smaller and the cloud response to warming weaker.

It is also interesting to compare with earlier studies, where LES simulations previously have suggested trade wind cumulus feedback in the range  $0.3$  and  $2.3 \text{ Wm}^{-2}\text{K}^{-1}$  (Bretherton, 2015; Nuijens and Siebesma, 2019), and observational studies up until recently likewise  $0.3$  -  $1.7 \text{ Wm}^{-2}\text{K}^{-1}$  (Klein et al., 2017). A recent observational study, however, finds a near-zero trade wind cumulus cloud feedback (Myers et al., submitted), which is in line with our results. It is perhaps tempting to think that other LES studies were under-resolved, that is, if they had been run with higher resolutions their estimated cloud feedback might have decreased. Although it seems likely that most LES will exhibit a similar resolution dependence of the cloud amount feedback to that found here, it is not clear why they should all converge to a near-zero total feedback given their differences in e.g. microphysics, and so no conclusions in this regard can be drawn here. It is, however, an interesting question for the community to address in the future.

*Code availability.* The ICON model source code is available for scientific use under an institutional or a personal non-commercial research license. Specific information on how to obtain the model code can be found under: [https://code.mpimet.mpg.de/projects/iconpublic/wiki/How\\_to\\_obtain\\_the\\_model\\_code](https://code.mpimet.mpg.de/projects/iconpublic/wiki/How_to_obtain_the_model_code).

*Author contributions.* The original idea of this study was conceived by CH and TM, whereas all simulations and most analysis was conducted

290 by JR. All authors contributed to the writing.

*Competing interests.* The authors declare that they have no conflict of interest.

*Acknowledgements.* This study was supported by the Max-Planck-Gesellschaft (MPG) and computational resources were made available by Deutsches Klimarechenzentrum (DKRZ) through support from Bundesministerium für Bildung und Forschung (BMBF). TM received funding from the European Research Council (grant no. 770765) ~~and~~ the H2020 European Research Council (grant no. **CONSTRAIN**

295 820829). This work was a contribution to the Cluster of Excellence 'CLICCS - Climate, Climatic Change, and Society', contribution to the Center for Earth System Research and Sustainability (CEN) of Universität Hamburg. This study benefitted from discussions and technical support from Guido Cioni and Tobias Becker. We thank the editor Johannes Quaas and two anonymous referees for their comments that helped to improve our manuscript.

## Appendix A: Initial profiles and large scale forcing

300 In the RICO case, van Zanten et al. (2011) constructed initial profiles as piecewise linear fits of radiosonde measurements up to a height of 4 km. As modification to the case defined by van Zanten et al. (2011), radiation is computed interactively to be able to calculate shortwave cloud radiative effects, which requires a model top at about 20 km in ICON-LEM. Below 4 km height, initial profiles as in van Zanten et al. (2011) are applied, above they are expanded accordingly, mostly with piecewise linear extrapolation, see Table A1 for details. The free tropospheric lapse rate  ~~$\frac{d\theta}{dz}$  is calculated with~~

305 
$$\frac{d\theta}{dz} = \frac{Q_R}{w(z)},$$

~~where is chosen such that~~ the imposed subsidence ~~w-warming~~ balances a radiative cooling  $Q_R$  of  $2.5 \text{ K day}^{-1}$  as suggested in the RICO setup. The temperature profile thus follows roughly a moist adiabat in the lower free troposphere. At 17 km, a tropopause of 195 K is included. The specific humidity profile is calculated from relative humidity following a linear decrease from 20% at 4 km height to 1% at 15 km and 0% at 17 km height.

**Table A1.** Fixed points for piecewise linear profiles of  $\theta$ ,  $q_v$ ,  $u$ ,  $v$ , the subsidence rate  $W$  and the large scale forcing of heat  $\partial_t \theta|_{LS}$  and moisture  $\partial_t q_v|_{LS}$  extended from the RICO case (van Zanten et al., 2011), from 4 km to 22 km height.

Height m	$\theta$ K	$q_v$ $\text{kg kg}^{-1}$	$u$ $\text{ms}^{-1}$	$v$ $\text{ms}^{-1}$	$W$ $\text{ms}^{-1}$	$\partial_t q_v _{LS}$ $\text{g kg}^{-1} \text{day}^{-1}$	$\partial_t \theta _{LS}$ $\text{K day}^{-1}$
0	297.9	0.016	-3.8	-9.9	0	-1.0	-2.5
740	297.9	0.0138					
2260	306.8				-0.005		
2980						0.3456	
3260		0.0024					
4000		0.0018		-1.9	-0.005	0.3456	
5000					-0.007		
7000	(AI)	$q(rh)$				0.13824	
10000						0.03456	
12000				16.1	-0.007		-2.5
15000		$q(rh=1)$				0	
17000	381.03	0			0	0	-0.4
22000		0	-3.8	-1.9	0		0

### 310 Appendix B: Impact of domain size

In order to confidently link the observed differences to characteristics of the resolution and not of the domain size, a simulation at the same horizontal resolution (1 km) is performed on two different domain sizes (50 km and 500 km). The simulations show that differences between the cloud field on the two domains are small (Fig. B1). With larger domain size, clouds are slightly deeper and show a narrower cloud fraction profile; total cloud cover is 1% points less (1 km resolution). On the same domain,  
315 the cloud cover would hence be even larger with the coarser resolutions.

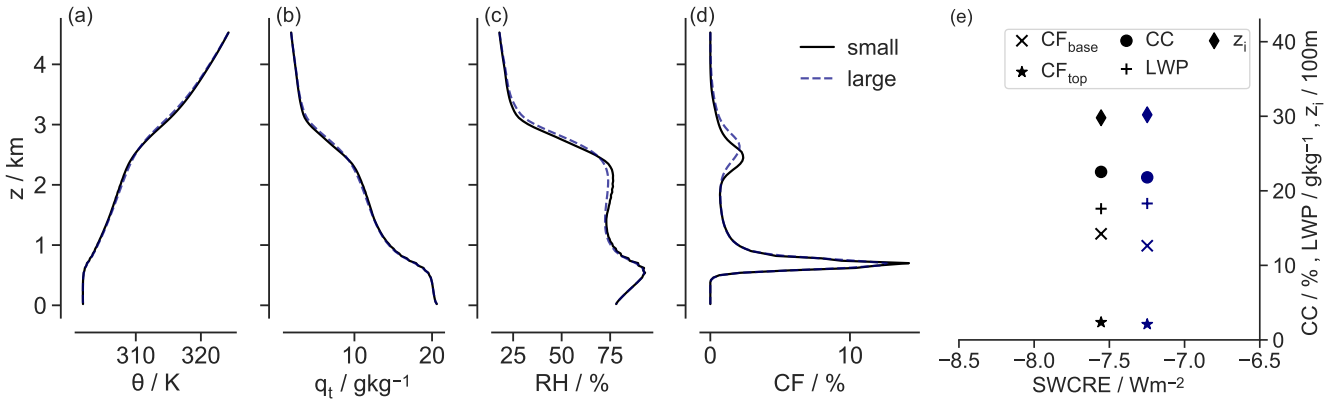


**Figure B1.** Profiles of second day domain averaged (a) potential temperature  $\theta$ , (b) specific humidity  $q_t$ , (c) relative humidity  $RH$  and (d) cloud fraction  $CF$ ; as well as (e) mean values of total cloud cover ( $CC$ ), cloud fraction at base ( $CF_{\text{base}}$ ) and top ( $CF_{\text{top}}$ ), liquid water path ( $LWP$ ) and inversion height ( $z_i$ ) at 1 km resolution on two different domain sizes:  $50 \times 50 \text{ km}$  (black, small) and  $500 \times 500 \text{ km}$  (blue-dashed, large).

## References

Albrecht, B. A.: Effects of precipitation on the thermodynamic structure of the trade wind boundary layer, *Journal of Geophysical Research*, <https://doi.org/10.1029/93JD00027>, 1993.

Blossey, P. N., Bretherton, C. S., and Wyant, M. C.: Subtropical Low Cloud Response to a Warmer Climate in a Superparameterized Climate Model. Part II: Column Modeling with a Cloud Resolving Model, *Journal of Advances in Modeling Earth Systems*, 1, <https://doi.org/https://doi.org/10.3894/JAMES.2009.1.8>, <https://agupubs.onlinelibrary.wiley.com/doi/abs/10.3894/JAMES.2009.1.8>, 2009.

Blossey, P. N., Bretherton, C. S., Zhang, M., Cheng, A., Endo, S., Heus, T., Liu, Y., Lock, A. P., de Roode, S. R., and Xu, K.-M.: Marine low cloud sensitivity to an idealized climate change: The CGILS LES intercomparison, *Journal of Advances in Modeling Earth Systems*, 5, 234–258, <https://doi.org/10.1002/jame.20025>, 2013.

Bony, S. and Dufresne, J.-L.: Marine boundary layer clouds at the heart of tropical cloud feedback uncertainties in climate models, *Geophysical Research Letters*, 32, <https://doi.org/10.1029/2005GL023851>, <https://agupubs.onlinelibrary.wiley.com/doi/full/10.1029/2005GL023851>, 2005.

Boucher, O., Randall, D., Artaxo, P., Bretherton, C., Feingold, G., Forster, P., Kerminen, V., Kondo, Y., H., L., and et al Lohmann U, e. a. : Clouds and Aerosols, in: *Climate change 2013: the physical science basis. Contribution of working group I to the fifth assessment report of the intergovernmental panel on climate change*, vol. 5, pp. 571–658, Cambridge University Press, Cambridge, <https://doi.org/10.1017/CBO9781107415324.016>, 2013.

Bretherton, C. S.: Insights into low-latitude cloud feedbacks from high-resolution models, *Philosophical transactions of the Royal Society A*, 373, <https://doi.org/10.1098/rsta.2014.0415>, 2015.

335 Bretherton, C. S., Blossey, P. N., and Jones, C. R.: Mechanisms of marine low cloud sensitivity to idealized climate perturbations: A single-LES exploration extending the CGILS cases, *Journal of Advances in Modeling Earth Systems*, 5, 316–337, <https://doi.org/10.1002/jame.20019>, 2013.

Brient, F. and Bony, S.: Interpretation of the positive low-cloud feedback predicted by a climate model under global warming, *Climate Dynamics*, 40, 2415–2431, <https://doi.org/10.1007/s00382-011-1279-7>, 2013.

340 Brient, F., Schneider, T., Tan, Z., Bony, S., Qu, X., and Hall, A.: Shallowness of tropical low clouds as a predictor of climate models' response to warming, *Climate Dynamics*, 47, 433–449, <https://doi.org/10.1007/s00382-015-2846-0>, 2015.

Cheng, A., Xu, K.-M., and Stevens, B.: Effects of Resolution on the Simulation of Boundary-layer Clouds and the Partition of Kinetic Energy to Subgrid Scales, *Journal of Advances in Modeling Earth Systems*, 2, [https://doi.org/https://doi.org/10.3894/JAMES.2010.2.3](https://doi.org/10.3894/JAMES.2010.2.3), <https://agupubs.onlinelibrary.wiley.com/doi/abs/10.3894/JAMES.2010.2.3>, 2010.

345 Dipankar, A., Stevens, B., Heinze, R., Moseley, C., Zängl, G., Giorgetta, M., and Brdar, S.: Large eddy simulation using the general circulation model ICON, *Journal of Advances in Modeling Earth Systems*, 7, 963–986, <https://doi.org/10.1002/2015MS000431>, 2015.

Doms, G., Förstner, J., Heise, E., Herzog, H. J., Mironov, D., Raschendorfer, M., Reinhardt, T., Ritter, B., Schrödin, R., Schulz, J.-P., and Vogel, G.: A description of the nonhydrostatic regional COSMO model part II: physical parameterization., Deutscher Wetterdienst: Offenbach, Germany, [http://www.cosmo-model.org/content/model/documentation/core/cosmo\\_physics\\_4.20.pdf](http://www.cosmo-model.org/content/model/documentation/core/cosmo_physics_4.20.pdf), 2011.

350 Flynn, C. M. and Mauritsen, T.: On the climate sensitivity and historical warming evolution in recent coupled model ensembles, *Atmospheric Chemistry and Physics*, 20, 7829–7842, <https://doi.org/10.5194/acp-20-7829-2020>, <https://acp.copernicus.org/articles/20/7829/2020/>, 2020.

Hartmann, D. L., Ockert-Bell, M. E., and Michelsen, M. L.: The Effect of Cloud Type on Earth's Energy Balance: Global Analysis, *Journal of Climate*, 5, 1281–1304, [https://doi.org/10.1175/1520-0442\(1992\)005<1281:TEOCTO>2.0.CO;2](https://doi.org/10.1175/1520-0442(1992)005<1281:TEOCTO>2.0.CO;2), 1992.

355 Heinze, R., Dipankar, A., Henken, C. C., Moseley, C., Sourdeval, O., Trömel, S., Xie, X., Adamidis, P., Ament, F., Baars, H., Barthlott, C., Behrendt, A., Blahak, U., Bley, S., Brdar, S., Brueck, M., Crewell, S., Deneke, H., Di Girolamo, P., Evaristo, R., Fischer, J., Frank, C., Friederichs, P., Göcke, T., Gorges, K., Hande, L., Hanke, M., Hansen, A., Hege, H.-C., Hoose, C., Jahns, T., Kalthoff, N., Klocke, D., Kneifel, S., Knippertz, P., Kuhn, A., van Laar, T., Macke, A., Maurer, V., Mayer, B., Meyer, C. I., Muppa, S. K., Neggers, R. A. J., Orlandi, E., Pantillon, F., Pospichal, B., Röber, N., Scheck, L., Seifert, A., Seifert, P., Senf, F., Siligam, P., Simmer, C., Steinke, S., Stevens, B., Wapler, K., Weniger, M., Wulfmeyer, V., Zängl, G., Zhang, D., and Quaas, J.: Large-eddy simulations over Germany using ICON: a comprehensive evaluation, *Quarterly Journal of the Royal Meteorological Society*, 143, 69–100, <https://doi.org/10.1002/qj.2947>, 2017.

Hohenegger, C., Kornblueh, L., Klocke, D., Becker, T., Cioni, G., Engels, J. F., Schulzweida, U., and Stevens, B.: Climate statistics in global simulations of the atmosphere, from 80 to 2.5 km grid spacing, *Journal of the Meteorological Society of Japan*, 98, 73–91, <https://doi.org/10.2151/jmsj.2020-005>, 2020.

360 Klein, S. A., Hall, A., Norris, J. R., and Pincus, R.: Low-Cloud Feedbacks from Cloud-Controlling Factors: A Review, *Surveys in geophysics*, 38, 1307–1329, <https://doi.org/10.1007/s10712-017-9433-3>, <https://doi.org/10.1007/s10712-017-9433-3>, 2017.

Klocke, D., Brueck, M., Hohenegger, C., and Stevens, B.: Rediscovery of the doldrums in storm-resolving simulations over the tropical Atlantic, *Nature Geoscience*, 10, 891–896, <https://doi.org/10.1038/s41561-017-0005-4>, <https://www.nature.com/articles/s41561-017-0005-4.pdf>, 2017.

365 Mauritsen, T. and Roeckner, E.: Tuning the MPI-ESM1.2 Global Climate Model to Improve the Match With Instrumental Record Warming by Lowering Its Climate Sensitivity, *Journal of Advances in Modeling Earth Systems*, 12, e2019MS002037,

https://doi.org/https://doi.org/10.1029/2019MS002037, https://agupubs.onlinelibrary.wiley.com/doi/abs/10.1029/2019MS002037, e2019MS002037 10.1029/2019MS002037, 2020.

Medeiros, B., Stevens, B., and Bony, S.: Using aquaplanets to understand the robust responses of comprehensive climate models to forcing, 375 Climate Dynamics, https://doi.org/10.1007/s00382-014-2138-0, 2015.

Myers, T. A., Scott, R. C., Zelinka, M. D., A., K. S., and Norris, J. R.: Extreme model climate sensitivities inconsistent with constraints on low cloud feedback, -, submitted.

Nuijens, L. and Siebesma, A. P.: Boundary Layer Clouds and Convection over Subtropical Oceans in our Current and in a Warmer Climate, Current Climate Change Reports, 5, 80–94, https://doi.org/10.1007/s40641-019-00126-x, 2019.

380 Nuijens, L., Stevens, B., and Siebesma, A. P.: The Environment of Precipitating Shallow Cumulus Convection, Journal of the Atmospheric Sciences, 66, 1962–1979, https://doi.org/10.1175/2008JAS2841.1, 2009.

Nuijens, L., Serikov, I., Hirsch, L., Lonitz, K., and Stevens, B.: The distribution and variability of low-level cloud in the North Atlantic trades, Quarterly Journal of the Royal Meteorological Society, 140, 2364–2374, https://doi.org/10.1002/qj.2307, 2014.

Paltridge, G. W.: Cloud-radiation feedback to climate, Quarterly Journal of the Royal Meteorological Society, 106, 895–899, 385 https://doi.org/10.1002/qj.49710645018, https://rmets.onlinelibrary.wiley.com/doi/abs/10.1002/qj.49710645018, 1980.

Prein, A. F., Langhans, W., Fosser, G., Ferrone, A., Ban, N., Goergen, K., Keller, M., Tölle, M., Gutjahr, O., Feser, F., Brisson, E., Kollet, S., Schmidli, J., van Lipzig, N. P. M., and Leung, R.: A review on regional convection-permitting climate modeling: Demonstrations, prospects, and challenges, Rev. Geophys., 53, 323–361, https://doi.org/10.1002/2014RG000475, 2015.

Rauber, R. M., Stevens, B., Ochs, H. T., Knight, C., Albrecht, B. A., Blyth, A. M., Fairall, C. W., Jensen, J. B., Lasher-Trapp, S. G., Mayol-390 Bracero, O. L., Vali, G., Anderson, J. R., Baker, B. A., Bandy, A. R., Burnet, E., Brenguier, J.-L., Brewer, W. A., Brown, P. R. A., Chuang, R., Cotton, W. R., Di Girolamo, L., Geerts, B., Gerber, H., Göke, S., Gomes, L., Heikes, B. G., Hudson, J. G., Kollias, P., Lawson, R. R., Krueger, S. K., Lenschow, D. H., Nuijens, L., O’Sullivan, D. W., Rilling, R. A., Rogers, D. C., Siebesma, A. P., Snodgrass, E., Stith, J. L., Thornton, D. C., Tucker, S., Twohy, C. H., and Zuidema, P.: Rain in Shallow Cumulus Over the Ocean: The RICO Campaign, Bulletin of the American Meteorological Society, 88, 1912–1928, https://doi.org/10.1175/BAMS-88-12-1912, 2007.

395 Rieck, M., Nuijens, L., and Stevens, B.: Marine Boundary Layer Cloud Feedbacks in a Constant Relative Humidity Atmosphere, Journal of the Atmospheric Sciences, 69, 2538–2550, https://doi.org/10.1175/JAS-D-11-0203.1, 2012.

Satoh, M., Stevens, B., Judt, F., Khairoutdinov, M., Lin, S.-J., Putman, W. M., and Düben, P.: Global Cloud-Resolving Models, Current Climate Change Reports, 5, 172–184, https://doi.org/10.1007/s40641-019-00131-0, 2019.

400 Sherwood, S. C., Webb, M. J., Annan, J. D., Armour, K. C., Forster, P. M., Hargreaves, J. C., Hegerl, G., Klein, S. A., Marvel, K. D., Rohling, E. J., Watanabe, M., Andrews, T., Braconnot, P., Bretherton, C. S., Foster, G. L., Hausfather, Z., von der Heydt, A. S., Knutti, R., Mauritsen, T., Norris, J. R., Proistosescu, C., Rugenstein, M., Schmidt, G. A., Tokarska, K. B., and Zelinka, M. D.: An Assessment of Earth’s Climate Sensitivity Using Multiple Lines of Evidence, Reviews of Geophysics, 58, e2019RG000678, https://doi.org/https://doi.org/10.1029/2019RG000678, https://agupubs.onlinelibrary.wiley.com/doi/abs/10.1029/2019RG000678, e2019RG000678 2019RG000678, 2020.

405 Siebesma, A. P., Bretherton, C. S., Brown, A., Chlond, A., Cuxart, J., Duynkerke, P. G., Jiang, H., Khairoutdinov, M., Lewellen, D., Moeng, C.-H., Sanchez, E., Stevens, B., and Stevens, D. E.: A Large Eddy Simulation Intercomparison Study of Shallow Cumulus Convection, Journal of the Atmospheric Sciences, 60, 1201–1219, https://doi.org/10.1175/1520-0469(2003)60<1201:ALESIS>2.0.CO;2, 2003.

Stevens, B.: On the Growth of Layers of Nonprecipitating Cumulus Convection, Journal of the Atmospheric Sciences, 64, 2916–2931, https://doi.org/10.1175/JAS3983.1, 2007.

410 Stevens, B., Ackerman, A. S., Albrecht, B. A., Brown, A. R., Chlond, A., Cuxart, J., Duynkerke, P. G., Lewellen, D. C., Macvean, M. K., Neggers, R. A. J., Sánchez, E., Siebesma, A. P., and Stevens, D. E.: Simulations of Trade Wind Cumuli under a Strong Inversion, *Journal of the Atmospheric Sciences*, 58, 1870–1891, [https://doi.org/10.1175/1520-0469\(2001\)058<1870:SOTWCU>2.0.CO;2](https://doi.org/10.1175/1520-0469(2001)058<1870:SOTWCU>2.0.CO;2), 2001.

415 Stevens, B., Satoh, M., Auger, L., Biercamp, J., Bretherton, C. S., Chen, X., Düben, P., Judt, F., Khairoutdinov, M., Klocke, D., Kodama, C., Kornblueh, L., Lin, S. J., Neumann, P., Putman, W. M., Röber, N., Shibuya, R., Vanniere, B., Vidale, P. L., Wedi, N., and Zhou, L.: DYAMOND: the DYnamics of the Atmospheric general circulation Modeled On Non-hydrostatic Domains, *Progress in Earth and Planetary Science*, <https://doi.org/10.1186/s40645-019-0304-z>, 2019.

420 Stevens, B., Acquistapace, C., Hansen, A., Heinze, R., Klinger, C., Klocke, D., Rybka, H., Schubotz, W., Windmiller, J., Adamidis, P., Arka, I., Barlakas, V., Biercamp, J., Brueck, M., Brune, S., Buehler, S. A., Burkhardt, U., Cioni, G., Costa-Surós, M., Crewell, S., Crüger, T., Deneke, H., Friederichs, P., Henken, C. C., Hohenegger, C., Jacob, M., Jakub, F., Kalthoff, N., Köhler, M., van LAAR, T. W., Li, P., Löhner, U., Macke, A., Madenach, N., Mayer, B., Nam, C., Naumann, A. K., Peters, K., Poll, S., Quaas, J., Röber, N., Rochetin, N., Scheck, L., Schemann, V., Schnitt, S., Seifert, A., Senf, F., Shapkaljevski, M., Simmer, C., Singh, S., Sourdeval, O., Spickermann, D., Strandgren, J., Tessiot, O., Vercauteren, N., Vial, J., Voigt, A., and Zängl, G.: The added value of large-eddy and storm-resolving models for simulating clouds and precipitation, *Journal of the Meteorological Society of Japan*, 98, 395–435, <https://doi.org/10.2151/jmsj.2020-021>, 2020.

425 Tomita, H.: A global cloud-resolving simulation: Preliminary results from an aqua planet experiment, *Geophysical Research Letters*, 32, 3283, <https://doi.org/10.1029/2005GL022459>, 2005.

430 van Zanten, M. C., Stevens, B., Nuijens, L., Siebesma, A. P., Ackerman, A. S., Burnet, F., Cheng, A., Couvreux, F., Jiang, H., Khairoutdinov, M., Kogan, Y., Lewellen, D. C., Mechem, D., Nakamura, K., Noda, A., Shipway, B. J., Slawinska, J., Wang, S., and Wyszogrodzki, A.: Controls on precipitation and cloudiness in simulations of trade-wind cumulus as observed during RICO, *Journal of Advances in Modeling Earth Systems*, 3, n/a–n/a, <https://doi.org/10.1029/2011MS000056>, 2011.

435 Vial, J., Dufresne, J.-L., and Bony, S.: On the interpretation of inter-model spread in CMIP5 climate sensitivity estimates, *Climate Dynamics*, 41, 3339–3362, <https://doi.org/10.1007/s00382-013-1725-9>, 2013.

440 Vial, J., Bony, S., Dufresne, J.-L., and Roehrig, R.: Coupling between lower-tropospheric convective mixing and low-level clouds: Physical mechanisms and dependence on convection scheme, *Journal of advances in modeling earth systems*, 8, 1892–1911, <https://doi.org/10.1002/2016MS000740>, 2016.

Vogel, R., Nuijens, L., and Stevens, B.: The role of precipitation and spatial organization in the response of trade-wind clouds to warming, *Journal of Advances in Modeling Earth Systems*, 8, 843–862, <https://doi.org/10.1002/2015MS000568>, 2016.

Webb, M. J., Senior, C. A., Sexton, D. M., Ingram, W. J., Williams, K. D., Ringer, M. A., McAvaney, B. J., Colman, R., Soden, B. J., Gudgel, R., Knutson, T., Emori, S., Ogura, T., Tushima, Y., Andronova, N., Li, B., Musat, I., Bony, S., and Taylor, K. E.: On the contribution of local feedback mechanisms to the range of climate sensitivity in two GCM ensembles, <https://doi.org/10.1007/s00382-006-0111-2>, 2006.

Zelinka, M. D., Zhou, C., and Klein, S. A.: Insights from a refined decomposition of cloud feedbacks, *Geophysical Research Letters*, 43, 9259–9269, <https://doi.org/10.1002/2016GL069917>, 2016.

Zelinka, M. D., Myers, T. A., McCoy, D. T., Po-Chedley, S., Caldwell, P. M., Ceppi, P., Klein, S. A., and Taylor, K. E.: Causes of Higher Climate Sensitivity in CMIP6 Models, *Geophysical Research Letters*, 47, e2019GL085782, <https://doi.org/10.1029/2019GL085782>, 10.1029/2019GL085782, 2020.